A&A 508, 289–295 (2009)
DOI: 10.1051/0004-6361/200912469

Astronomy & Astrophysics

Li-rich red giant branch stars in the Galactic bulge

O. A. Gonzalez[1,2], M. Zoccali[1], L. Monaco[3], V. Hill[4], S. Cassisi[5], D. Minniti[1,6], A. Renzini[7], B. Barbuy[8], S. Ortolani[9], and A. Gomez[10]

[1] Departamento Astronomía y Astrofísica, Pontificia Universidad Católica de Chile, Av. Vicuña Mackenna 4860 Stgo., Chile
e-mail: oagonzal@uc.cl; [mzoccali;Dante]@astro.puc.cl
[2] European Southern Observatory, Karl-Schwarzschild-Strasse 2, 85748 Garching, Germany
[3] Departamento Ciencias Físicas y Astronómicas, Universidad de Concepción, Concepción, Chile
[4] Université de Nice Sophia Antipolis, CNRS, Observatoire de la Côte d'Azur, BP 4229, 06304 Nice Cedex 4, France
[5] INAF-Osservatorio Astronomico di Teramo, via M. Maggini, 64100 Teramo, Italy
[6] Specola Vaticana, V00120 Citta del Vaticano, Italy
[7] INAF-Osservatorio Astronomico di Padova, Vicolo dell'Osservatorio 2, 35122 Padova, Italy
[8] Universidade de São Paulo, IAG, Rua do Matão 1226, Cidade Universitária, São Paulo 05508-900, Brazil
[9] Università di Padova, Dipartimento di Astronomia, Vicolo dell'Osservatorio 5, 35122 Padova, Italy
[10] Observatoire de Paris-Meudon, 92195 Meudon Cedex, France

Received 11 May 2009 / Accepted 9 July 2009

ABSTRACT

Aims. We present lithium abundance determination for a sample of K giant stars in the Galactic bulge. The stars presented here are the only 13 stars with a detectable lithium line (6767.18 Å) among ~400 stars for which we have spectra in this wavelength range, half of them in Baade's Window ($b = -4°$) and half in a field at $b = -6°$.
Methods. The stars were observed with the GIRAFFE spectrograph of FLAMES mounted on VLT, with a spectral resolution of $R \sim 20\,000$. Abundances were derived from spectral synthesis and the results are compared with those of stars with similar parameters, but no detectable Li line.
Results. We find 13 stars with a detectable Li line, among which 2 have abundances $A(\mathrm{Li}) > 2.7$. No clear correlations were found between the Li abundance and those of other elements. With the exception of the two most Li rich stars, the others follow a fairly tight $A(\mathrm{Li}) - T_{\rm eff}$ correlation.
Conclusions. There is strong indication of a Li production phase during the red giant branch (RGB), acting either on a very short timescale, or selectively only in some stars. That the proposed Li production phase is associated with the RGB bump cannot be excluded, although our targets are significantly brighter than the predicted RGB bump magnitude for a population at 8 kpc.

Key words. stars: abundances – stars: late-type – Galaxy: bulge

1. Introduction

The cosmic evolution of lithium has been hotly debated because of some marked inconsistencies between its predicted abundance and a few key observations (see, e.g., Cyburt et al. 2008, for a review).

The dominant lithium isotope is ^{7}Li, which is assumed to be produced by Big Bang nucleosynthesis, up to an abundance $A(\mathrm{Li}) \sim 2.2$, i.e., the so-called Spite plateau abundance observed in the surface of metal-poor stars. Since then, Li has been produced by hot bottom burning (Sackmann & Boothroyd 1999) during the asymptotic giant branch (AGB) evolution of intemediate mass stars (>4 $M_\odot$), or by cosmic ray spallation, but also destroyed in stellar interiors where tempratures are in excess of 2.0×10^6 K.

In this context, a typical bulge star of roughly solar metallicity is expected to begin its life, on the main sequence, with a Li abundance close to $A(\mathrm{Li}) = 3.0$. During the first dredge up, when envelope convection penetrates to high temperature regions, Li is partly destroyed (diluted) by ~1.5 dex (Iben 1967a,b), so that typical near solar metallicity RGB stars are expected to have $A(\mathrm{Li}) < 1.5$. However, stars on the upper RGB are expected to be more Li depleted because of the extra-mixing observed to occur during the RGB bump (Gratton et al. 2000; Lind et al. 2009b). In marked contrast to this expectation, several Li-rich red giants have been found, in both clusters and the field (e.g., McKellar 1940; Faraggiana 1991; Smith et al. 1995; Hill & Pasquini 1999; Kraft & Shetrone 2000; Domínguez et al. 2004; Uttenthaler et al. 2007; Monaco & Bonifacio 2008).

As a possible explanation of these results, a Li production phase during the RGB that emplays the Cameron-Fowler mechanism (Cameron & Fowler 1971) has been proposed (Sackmann & Boothroyd 1999; Charbonnel & Balachandran 2000; Denissenkov & Herwig 2004). To synthetize Li in stellar interiors, two conditions are required. First, temperatures should be hot enough for the reaction $^3\mathrm{He}(\alpha,\gamma)^7\mathrm{Be}$ to occur. Secondly, ^{7}Be must be quickly transported to cooler regions, where Li can be then produced by the $^7\mathrm{Be}(\mathrm{e}^-,\nu)^7\mathrm{Li}$ reaction. Thus, the reaction producing Be should occur very close to a convective region, or, alternatively, convection should penetrate into some burning shell. Then, in low mass stars, some kind of extra-mixing must circulate the material from the convective envelope to a region close to the H-burning shell. The source of this extra-mixing has been proposed to be e.g., shear inestabilities, meridional circulation, or diffusion.

Charbonnel & Balachandran (2000) show that a significant number of Li rich giants appear to be located close to

the RGB bump where an extra-mixing process is observed to strongly affect the abundances of C, $^{12}C/^{13}C$, and N (Gratton et al. 2000, 2004). Based on this evidence, they propose a scenario where, while the H-burning shell erases the molecular weight discontinuity left by the penetration of the convective envelope during the first dredge up, the extra-mixing could circulate the material to produce Li. When mixing has proceeded long enough to produce the observed dip in the carbon isotopic ratio during and after the RGB bump, the fresh ^{7}Li should be quickly destroyed, such that the Li rich phase would be a very short one. This latter point would explain why only a small fraction of the observed RGB stars are actually Li rich. However, this qualitative explanation has not been reproduced to date by models accounting for rotational distortions (Palacios et al. 2006) and is also challenged by some observations of Li rich stars significantly brighter than the RGB bump (Kraft et al. 1999; Uttenthaler et al. 2007; Monaco & Bonifacio 2008)

Sackmann & Boothroyd (1999) suggested that, under certain conditions, an increase in the Li abundance could be produced by a deep circulation mechanism after the molecular weight barrier is erased. Therefore, depending on the extra-mixing details, Li-rich red giants may be found at any location of the RGB. However, problems arise when the behavior of other elements are compared with the expected values from their proposed model. In particular, in their scenario the lower $^{12}C/^{13}C$ value is only reached at the tip of the RGB and not immediately after the RGB bump as observed (Gratton et al. 2004).

Alternatively, Denissenkov & Herwig (2004) proposed a distinction between the extra-mixing at the RGB bump and a so-called enhanced extra-mixing induced by rotation that could be triggered by the spinning up by an external source of angular momentum, which could then increase the Li abundance.

Other explanations of Li-rich red giants have been proposed, such as some mechanism that might prevent Li dilution during the first dredge up, or contamination by possible planets. However, both phenomena would involve some enrichment of ^{9}Be (in addition to ^{6}Li and ^{11}B), which is not usually observed in Li-rich stars (Melo et al. 2006). Therefore, the internal Li production during the RGB via the Cameron-Fowler mechanism seems to be the most likely scenario for explaining low mass Li-rich giants.

Two different sources of extra mixing have been proposed to reproduce the observed changes in surface abundances. Thermohaline mixing triggered by a double diffusive instability (Charbonnel & Zahn 2007a) and magneto-thermohaline mixing (Denissenkov et al. 2009) induced by magnetic buoyancy. While the way in which thermohaline mixing may account for observed Li rich giants has not yet been explained, Guandalini et al. (2009) showed that mixing induced by magnetic buoyancy might explain the observation of both Li-rich and Li-poor stars along the RGB. However, a deeper understanding of magnetic fields in low mass giants as well as a larger sample of Li rich RGB stars are required to confirm these results.

Here, we present Li abundances of 13 stars with detectable Li spectral lines, observed in the context of our survey of RGB stars in the Galactic bulge (see Zoccali et al. 2008; and Lecureur et al. 2007, for a description of the entire project).

2. RGB sample

The spectra discussed here were obtained as part of a larger FLAMES-GIRAFFE survey of bulge K giants, in four fields (cf. Zoccali et al. 2008). Only two of the fields, namely Baade's window and the field at $b = -6°$ were observed with the HR15 setup,

Table 1. Bulge field characteristics.

N	Name	l	b	R_{GC}	$E(B-V)$
1	Baade's Window	1.14	−4.18	604	0.55
2	$b = -6°$	0.21	−6.02	850	0.48

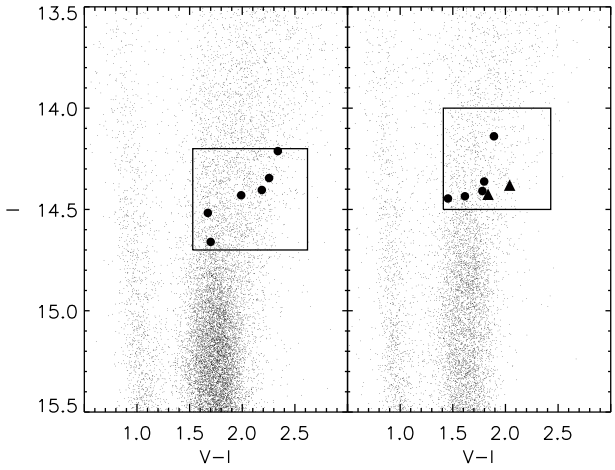

Fig. 1. Color magnitude diagram for both fields, Baade's window (*left*) and $b = -6$ (*right*) with the positions of the Li-rich stars in our sample marked as large filled circles. The two stars with the highest Li abundances are marked as large filled triangles. Magnitudes were obtained from the OGLE catalogue (Udalski et al. 2002) and the Zoccali et al. (2008) catalogue obtained from WFI images.

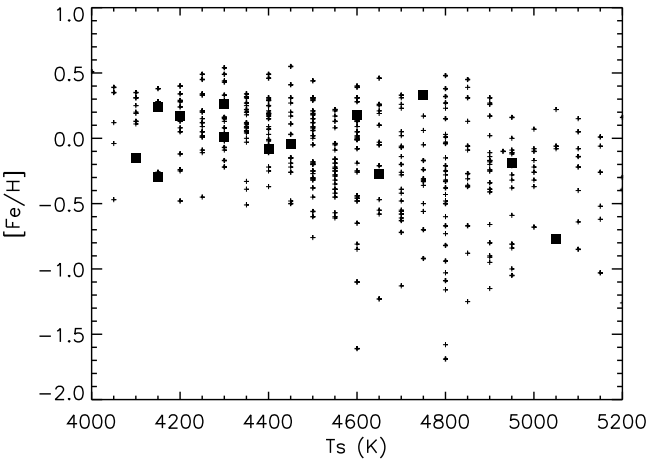

Fig. 2. Metallicity versus effective temperature diagram for all the observed bulge giants (small crosses) in both fields. Li rich giants are shown as big filled squares.

including the Li line at 6707.18 Å. The S/N ranges from 40 to 90 and the resolution is $R \sim 20\,000$. In total, we measured Li in 204 + 213 = 417 bulge giants, whose location in the color magnitude diagram (CMD) is shown in Fig. 1. For only 13 of these stars was there a detectable Li line, thus the following analysis concentrates on these stars, which we refer to as "Li rich" stars[1].

Stellar parameters were obtained from Zoccali et al. (2008). As can be seen from Fig. 2, observed stars have effective temperatures varying from 4000 to 5200 K and an iron content, [Fe/H], between −1.7 and +0.5. Li-rich stars span the entire temperature

[1] Note that the name "Li rich" has been often used for giants with A(Li) > 1.5. Only 6 of our stars have such a high abundance, but we extend the name here to all stars with detectable Li in our sample, in contrast to the other ~400 giants for which we could see no line at all.

Table 2. Atomic linelist in the vicinity of the lithium line, used for this study.

λ (Å)	Element	Xiex	log gf
6707.4331	Fe I	4.610	–2.300
6707.4500	Sm II	0.930	–3.140
6707.5630	V I	2.740	–1.530
6707.6440	Cr I	4.210	–2.140
6707.7400	Ce II	0.500	–3.810
6707.7520	Ti I	4.050	–2.654
6707.7561	^{7}Li	0.000	–0.428
6707.7682	^{7}Li	0.000	–0.206
6707.7710	Ca I	5.800	–4.015
6707.9066	^{7}Li	0.000	–1.509
6707.9080	^{7}Li	0.000	–0.807
6707.9187	^{7}Li	0.000	–0.807
6707.9200	^{7}Li	0.000	–0.807
6708.0250	Ti I	1.880	–4.252
6708.1001	V I	1.220	–3.200
6708.1250	Ti I	1.880	–2.886
6708.2800	V I	1.220	–3.178

range, while their rather high metallicity is consistent with ours being a small sample, randomly selected from the bulge metallicity distribution which is sharply peaked around solar.

3. Spectral synthesis and Li abundances

For the 13 stars for which there was a detectable line, Li abundances were determined by comparing with synthetic spectra created with MOOG (Sneden 2002). MOOG is a FORTRAN code that performs a spectral line analysis and spectrum synthesis assuming local thermal equilibrium. MARCS model atmospheres (Gustafsson 2008) were created using the stellar parameters given in Table 2.

3.1. Linelists

The TiO molecular line list (Plez 1998) used by Lecureur et al. (2007) was included, but those lines were found to be of negligible strength for the relevant wavelength range. CN lines are stronger, especially for cold stars. The Kurucz CN line list was obtained from the Kurucz database. Atomic lines in the vicinity of the Li line were obtained from Reddy et al. (2002).

Once all line lists were compiled, the log gf values of the CN and atomic lines within 8 Å of the Li line were modified to reproduce the observed spectra of Arcturus and μ Leonis, as shown in Fig. 3 using the abundances given in Lecureur et al. (2007). The log gf value for Ti I line at 6708.025 Å was modified from that adopted by Reddy et al. (2002) as well as both V I lines at 6708.125 Å and 6708.280 Å. The final, calibrated atomic lines used in the synthesis are listed in Table 2.

3.2. Synthesis

Synthetic spectra were computed for each Li rich star using the corresponding stellar parameters and iron content listed in Table 4. The abundances of C, N, and O were obtained from Lecureur et al. (2007), where, based on a subsample of stars observed at higher resolution with UVES, approximate relations were derived between the abundances of CNO and [Fe/H]. All other abundance ratios were scaled to the stellar metallicity assuming a solar mix (Grevesse & Sauval 1998). The observed

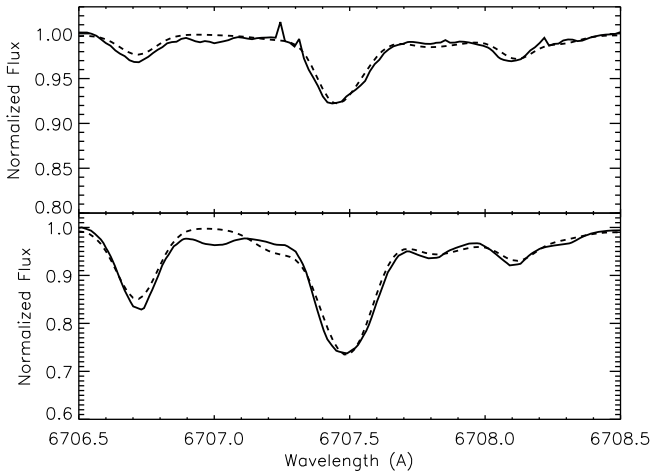

Fig. 3. Observed spectra as solid line and synthetic spectra as dashed line for Arcturus (*upper panel*) and for μ Leonis (*lower panel*) used for calibration of the log gf values for lines in the vecinity of the Li line.

spectra were corrected for the radial velocities obtained from DAOSPEC (Stetson & Pancino 2008) and checked for telluric lines in the Li wavelength range. Each synthetic spectrum was compared to the observed one in two steps. First, a 10 Å window was used to perform a correct normalization to the continuum around the Li line. Second, a smaller window (4 Å) was used to reproduce the Li line, iteratively modifying only the Li abundance until the best-fit model was identified. Additionally, NLTE corrections were calculated by interpolating within grids determined by Lind et al. (2009a,b), for the stellar parameters of each one of the Li-rich stars[2].

The derived LTE and NLTE Li abundances for the 13 Li rich stars are listed in the lasts two columns of Table 4. The two stars showing extremely high Li abundances, A(Li) $\sim$ 2.7, are showed in the left panels of Fig. 4 along with the best fitting synthetic spectrum. Additionally we performed spectral synthesis to other six stars from each field, spanning the whole parameter range of the Li rich sample, in order to obtain reference upper limit Li abundance for *normal* stars.

The errors on the measured Li abundances were obtained by varying each of the stellar parameters by its estimated error, and redetermining the Li abundance. The largest uncertainty is associated with the effective temperature, whose error is estimated to be ±200 K (Zoccali et al. 2008), implying a ΔA(Li) $\sim$ 0.25 dex for the hottest of our stars (see Table 3).

4. Possible origin of a high Li abundance

4.1. Correlations with temperature and metallicity

In an attempt to explain the high Li abundance measured for 13 of our stars, we investigate possible correlations between the derived Li content and the stellar parameters.

From the location of the Li rich stars in the CMD (Fig. 1), we see that they span the full color range of the other sample stars, and they also do not exhibit any clustering in magnitude space. This information, coupled with their uniform spatial distribution – and similar number in both fields – allows us to exclude that they might belong to a different, peculiar, stellar population, such as a star cluster.

[2] NLTE corrections in Lind et al. (2009a,b) are only available up to solar metallicity. Therefore, corrections for supersolar metallicity stars were calculated by assuming [Fe/H] = 0.

Table 3. Li abundance errors associated with the uncertainties in stellar parameters.

T	ΔT		$\Delta \log g$		Δv_t		Δ[Fe/H]	
(K)	−200 K	+200 K	−0.3 dex	+0.3 dex	−0.2 km s^{-1}	+0.2 km s^{-1}	−0.2 dex	+0.2 dex
4200	−0.15	0.20	−0.01	0.02	0.00	0.00	0.15	−0.14
4650	−0.20	0.20	−0.01	0.01	0.00	0.00	0.20	−0.16
4950	−0.25	0.25	−0.01	0.01	0.00	0.00	0.23	−0.25

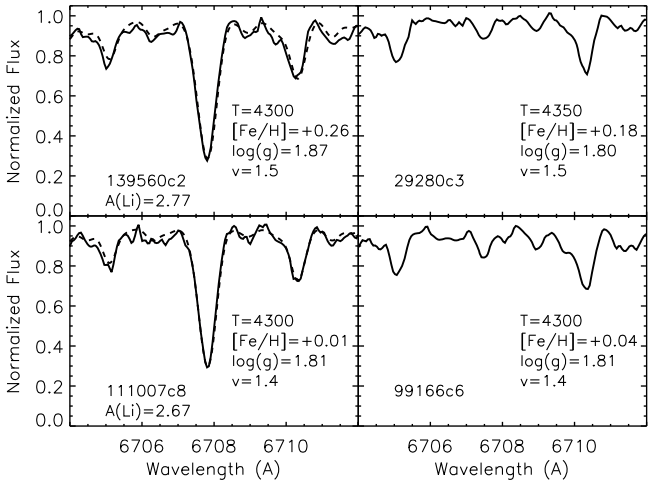

Fig. 4. *Left panels*: observed (solid line) and synthetic (dashed line) spectra for the two most Li-rich stars found from the sample. *Right panels*: observed spectra for two stars with similar $T_{\rm eff}$, [Fe/H], v_t, and $\log g$ to both Li-rich stars, but no ^{7}Li line present.

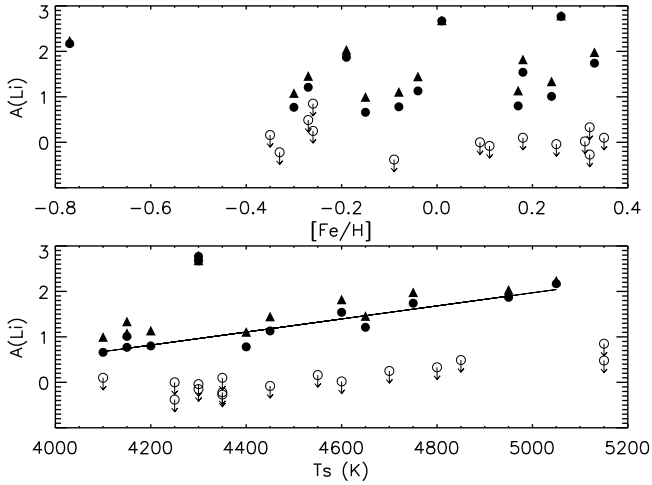

Fig. 5. Li_{LTE} (filled circles) and Li_{NLTE} (filled triangles) abundances and stellar parameters for the Li-rich stars. Upper limits to A(Li) for a sample of random stars are shown as empty circles. No correlation is seen between lithium abundances and metallicity (*upper panel*). A clear correlation is visible between A(Li) and $T_{\rm eff}$ (*lower panel*) with the only two outliers being the most Li rich stars. A linear fit to the data gives a slope of 0.14 ± 0.02 dex/100 K.

Table 4. Stellar parameters and determined Li abundance to the subsample of stars with a distinguishable Li line.

N	ID	$\log g$	v_t	T_s	[Fe/H]	$A(\mathrm{Li})_{\rm LTE}$	$A(\mathrm{Li})_{\rm NLTE}$
1	82831	1.99	1.4	4750	0.33	1.74	1.98
2	205356	2.16	1.5	4950	–0.19	1.87	2.04
3	564760	1.74	1.3	4150	–0.30	0.77	1.08
4	564789	1.70	1.2	4100	–0.15	0.66	1.00
5	231128	1.76	1.4	4200	0.17	0.80	1.14
6	392931	1.89	1.5	4450	–0.04	1.13	1.45
7	108191c7	2.11	1.5	5050	–0.77	2.17	2.24
8	69986c2	2.01	1.5	4650	–0.27	1.21	1.46
9	139560c2	1.87	1.5	4300	0.26	2.77	2.78
10	103413c6	1.65	1.4	4150	0.24	1.01	1.34
11	75601c7	1.79	1.5	4400	–0.08	0.78	1.11
12	77419c7	1.93	1.5	4600	0.18	1.54	1.82
13	111007c8	1.81	1.4	4300	0.01	2.67	2.68

All our Li-rich stars have metallicities in excess of [Fe/H] ∼ −0.3 with the exception of one star at [Fe/H] = −0.77 (Fig. 5). Given the global iron distribution function in these two fields (Zoccali et al. 2008), this is entirely consistent with (small) random sampling.

The temperature distribution of Li-rich stars is extremely uniform across the entire range sampled by our targets, from 4000 to 5200 K. Very interestingly, with the exception of the two extremely Li-rich stars shown in Fig. 4, all the other stars show a rather tight correlation between A(Li) and $T_{\rm eff}$, as already found by Brown et al. (1989) in a survey of 644 giants in the DDO photometric catalog, Pilachowski et al. (1986) in NGC 7789, and Pilachowski et al. (1988) for M 67 giants.

To confirm that the observed relation is real and not produced by a reduced sensitivity to Li detections at hotter temperatures (thereby introducing correlated errors in $T_{\rm eff}$ and A(Li)), we analyze here the possible effect of an error in temperature on the derived abundances.

Table 3 lists the variation in A(Li) caused by an error of 200 K in the temperature of the adopted model atmosphere. It appears that an increase in temperature would imply an increase in the derived A(Li), and vice versa, thus artificially introducing a positive slope in the lower panel of Fig. 5. According to Magain (1984), the slope produced by correlated errors would be given by

$$\langle \delta f \rangle = c \frac{\sigma_\gamma^2}{\sigma_T^2}$$

where: $c = \frac{\partial A(\mathrm{Li})}{\partial T} = 0.25$ dex/200 K describes how A(Li) is correlated with $T_{\rm eff}$, assuming the maximum variation, obtained for $T > 4950$; $\sigma_\gamma = 200$ K is the typical error in effective temperature; and $\sigma_T = 333$ K is the variance in the effective temperature range.

This infers an expected error in the slope that is due to correlated errors, of $\langle \delta f \rangle \sim 0.1$ dex/200 K. The best-fit relation for the data has a slope of 0.28 dex in 200 K. Therefore, most of the observed trend is certainly real.

The hypothesis proposed by Charbonnel & Balachandran (2000) implies that the RGB bump should act as the evolutive instance in which we can separate the stars into three groups according to their Li content: i) stars under standard dilution that should be less evolved than the RGB bump and therefore could show the observed trend in Fig. 5; ii) stars experiencing fresh Li production, which should be located at the first stages of the RGB bump before full mixing takes place; and iii) stars that have

left the RGB bump and for which no Li content should be observed on their surfaces. Thus, Li-rich stars should be located, in the CMD, very close to the RGB bump. However, our stars, being in principle significantly more evolved than RGB bump stars, obviously do not agree with this scenario. In this context, the observed decline in lithium with temperature observed in our stars, can only be interpreted as the result of a process occurring as they evolve through the giant branch.

4.2. The evolutionary status of the Li-rich stars

Two of the stars have A(Li) $\sim$ 2.7 and they are always above the observed trend. Similar abundances of Li were previously measured for two giants by Brown et al. (1989). According to Charbonnel & Balachandran (2000), the latter two stars belong to the RGB bump. Since they also showed Be and ^{6}Li depletion, they were interpreted as having recently undergone a Li production phase. Their normal ^{12}C/^{13}C ratios, imply that Li production should precede the extra-mixing process, lowering the carbon isotopic ratio. Our stars are brighter than the expected location of the RGB bump, if they are at the bulge mean distance. Therefore, the only way that they could be described by this scenario would be if they were far closer by, at ~5 kpc instead of 8 kpc (see below).

Our target selection box in the CMD is located about 0.7 mag above the horizontal branch red clump, at $V_{\rm box} \sim 16.1$. For a solar metallicity population, the expected $\Delta V_{\rm HB}^{\rm bump}$ is 0.5 mag (Zoccali et al. 1999). Since the observed red clump is at $V \sim$ 16.8, the RGB bump should then be at $V \sim 17.3$, i.e., 1.2 mag fainter than our target box. Even considering that the RGB bump occurs at brighter luminosities for metal-poor stars, not even for the most metal-poor, Li-rich star in our sample is the observed magnitude compatible with the expected location of the RGB bump. Assuming a mean bulge distance of 8 kpc, Li-rich stars in our sample should be at ~4.6 kpc from us to actually belong to the RGB bump. The bulge density at 3.4 kpc from the Galactic center is very low (Rattenbury et al. 2007). Therefore, although this possibility cannot be excluded, it is rather unlikely.

More likely, these stars might be *disk* RGB bump stars, at a distance of ~4.6 kpc. In principle, one way to separate bulge from disk stars might be on the basis of their alpha element abundances. It has been found that [α/Fe] ratios appear to be higher for bulge stars than those belonging to the disk (e.g., Zoccali et al. 2006; Lecureur et al. 2007). If oxygen cannot be measured at the resolution of GIRAFFE, we can measure Mg, Al, and Na and check whether they are lower than expected for bulge stars. Figure 6 shows that this is not the case, at least for Al and Na.

4.3. Binary nature

Costa et al. (2002) found that the Li abundances in binary systems including a giant show a trend with temperature similar to the one shown in Fig. 5. This was interpreted as being indicative of tidal interactions that influence standard dilution. Binary systems with synchronized rotational and orbital motions have higher lithium than to non-synchronized binaries. To check for binarity in our targets, we looked for radial velocity variations among the individual spectra, before co-addition. For each observed field, 6 to 8 individual spectra were obtained for different sub-samples, spanning a time window from 30 to 70 days. Star 108191c7 is the only one belonging to a sub-sample observed in only two nights. Figure 7 shows the radial velocity rms for the Li-rich stars, compared to stars with no Li line detected

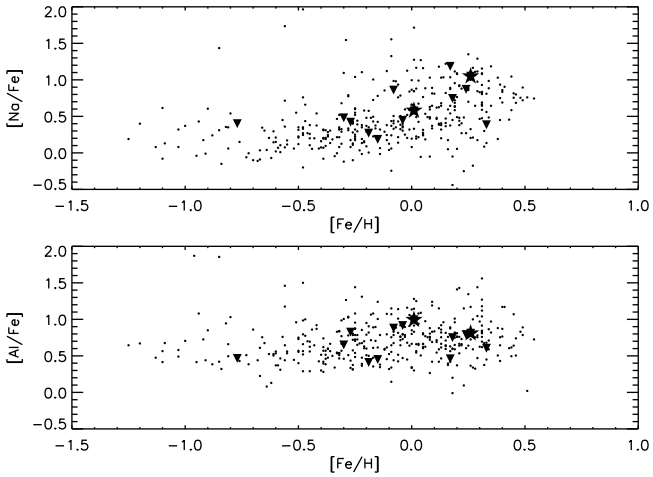

Fig. 6. [Na/Fe] and [Al/Fe] ratios versus metallicity. The full sample is ploted as small circles, the Li rich stars as filled triangles and the two most Li rich stars as filled stars.

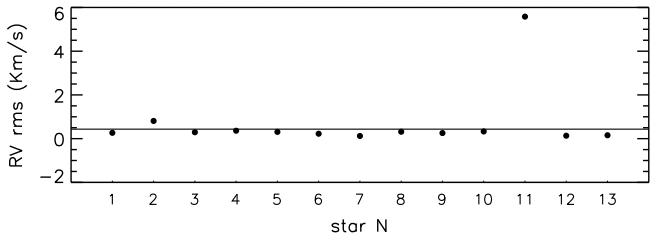

Fig. 7. Radial velocity variations of the Li rich stars (filled circles) compared to the mean variations of the rest of the sample (solid line).

(solid line). Only star 75601c7 shows variations of ~6 km s^{-1}, about 20 times higher than the others. Because of small sampling and projection effects, we cannot exclude that some other stars are binaries for which we do not detect the variations. However, once again, binarity for *all* the 13 stars would not seem to be the favoured scenario from the present data.

4.4. Circumstellar material and infrared excess

In the previous sections, we have demonstrated that the Li-rich stars we detect are most likely above the RGB bump. In agreement with this, Kraft et al. (1999) also detected an enhanced Li star in M3 (star IV-101 with A(Li) = 4.0) located 2.25 mag brighter than the RGB bump. Monaco & Bonifacio (2008) also found two stars with A(Li) > 3.5−4.0 close to the RGB tip of the Sagittarius dwarf spheroidal tidal stream.

De la Reza et al. (1996, 1997) proposed a different scenario for the Li production along the RGB, associated with short episodes of mass loss occurring just after each extra-mixing event. In this way, some fresh Li would be produced when convection penetrates close to the H-burning shell, which might occur at the RGB bump or brighter. The thin layer containing fresh Li would be quickly carried to the surface (and observed) but would be lost by the star immediately afterwards. Observational support of this scenario was given by the detection of infrared excess in some Li-rich giant stars (Gregorio-Hetem et al. 1993; De la Reza et al. 1996, 1997; Castilho et al. 1998).

Later on, however, Jasniewicz et al. (1999) analyzed 29 giants with an infrared excess and did not find any correlation with lithium abundance. In particular, most of their target stars had no detectable Li lines, 7 of them have abundances compatible with

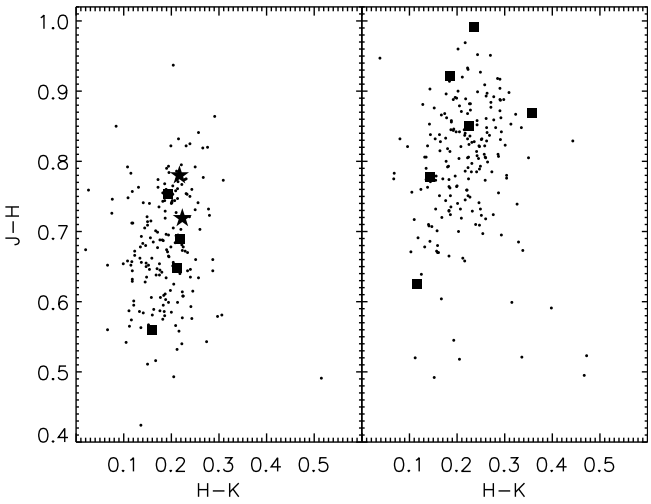

Fig. 8. ($J-H$, $H-K$) color−color diagram for the complete sample of stars in the $b = -6°$ field (*left*) and Baade's window (*right*) including the Li-rich stars (filled squares). The two most Li enhanced stars 139560c2 and 111007c8 are plotted as filled stars.

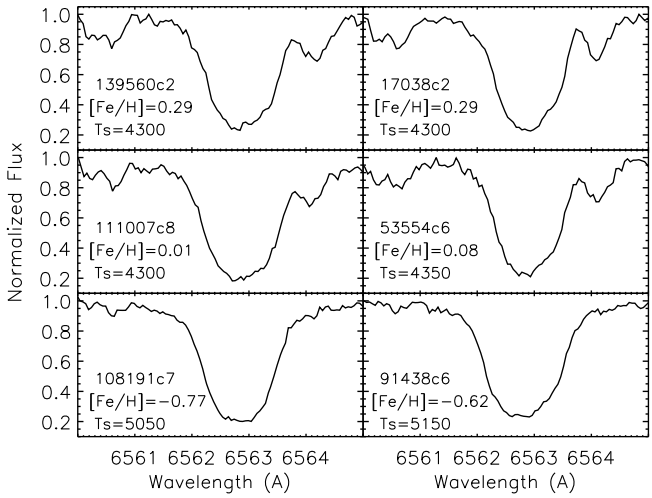

Fig. 9. H_α profile for 3 Li-rich (*left panels*) and 3 Li-poor (*right panel*) stars. There are no signs of chromospheric activity in the profiles, nor any other difference between Li-rich and Li-poor stars.

standard dilution (A(Li) ∼ 1.5), and only one has A(Li) = 3.0, the latter being indeed close to the RGB bump.

Ideally, mid or far infrared data are needed to detect an infrared excess. Since at the moment we do not have these data, we have examined the ($J-H$, $H-K$) color−color diagram to look for an excess K brightness. As shown by Jones (2008), stars with a clear excess flux ($\gtrsim$1 mag) at 8 μm with respect to K, also show a ∼0.4 mag excess brightness in $H-K$ with respect to no-IR-excess stars. Figure 8 shows that no near-IR excess is visible for any of the Li-rich stars compared to the bulk of normal stars in our sample. However, we note that this does not mean that these stars do not have circumstellar material. As shown by Origlia et al. (2007), moderate (∼0.5 mag) excess in $K-8$ μm is not detectable in the near IR.

Additionally, a significant number of Li-rich giants were also found to be rapid rotators (Drake et al. 2002). However, there is not a one-to-one relation between Li enrichment and rotation (de Medeiros et al. 1996). Furthermore, as found by Drake et al. (2002), this connection only seems to be present when high IR-excess is present. An indication of fast rotation ($v \sin i \gtrsim 8$ km s^{-1}) is observed as unusually broad lines in spectral features. In our case, measured FHWM of Li-rich stars show no enhancement when compared to the average of the sample.

Finally, were the high Li abundance related to circumstellar material, we could expect asymmetric wings and/or an emission component in the H_α line. Figure 9 shows that this is not observed, since the H_α lines of Li-rich stars (right panels) are identical to those of any other star in the sample (left panels).

5. Conclusions

We have analyzed the Li abundance of a sample of ∼400 K giants in the Galactic bulge. A subsample of 13 stars have detectable Li lines for which we have measured A(Li) = 0.7−2.8.

The sample stars could be divided into three categories:

i) ∼**Four hundred normal stars** showing no Li line.
ii) **Eleven Li-rich stars** with A(Li) = 0.66−1.87. These have abundances compatible with standard Li dilution ocurring at the 1st dredge up. However they seem to have somehow avoided the second extra-mixing episode, further diluting Li after the RGB bump (see Fig. 8 in the review by Gratton et al. 2004). These stars exhibit a clear correlation between A(Li) and $T_{\rm eff}$.
iii) **Two highly Li-rich stars** with A(Li) ∼ 2.8. These stars necessarily underwent a Li production phase.

Most of the proposed explanations for the presence of (a small fraction of) Li-rich RGB stars involve the Comeron-Fowler mechanism, associated with a deep mixing episode, occurring either at the RGB bump (Charbonnel & Balachandran 2000) or brighter (Sackmann & Boothroyd 1999; Denissenkov & Herwig 2004). From the position of our stars on the CMD, we conclude that it is rather unlikely that any of them belongs to the RGB bump, since they are observed to be ∼1.2 mag brighter than its expected position, at the mean bulge distance.

No clear indication has been found for the presence of a companion to these stars, nor for an infrared excess or some kind of chromospheric activity. By dividing the spectrum of Li-rich stars by one of a *normal* star with similar parameters, we were unable to identify any other spectral feature that might differ between the two spectra.

We have presented more evidence for the presence of Li-rich stars in the first ascent RGB, in contrast to the predictions of canonical stellar evolution. None of the proposed explanations could be confirmed here, even though some of them could not be firmly discarded either. Clearly, our poor understanding of this evidence is strongly affected by small number statistics, partly because of the intrinsec rareness of the phenomenon but also to the lack of a dedicated survey. Specifically designed observations would be needed, ideally in simple stellar populations, to establish clearly the evolutionary status of Li-rich giants.

Acknowledgements. We thank Alejandra Recio-Blanco, Angela Bragaglia and Patrick de Laverny for very useful comments and discussions. O.G. thanks Karin Lind for providing us with the interpolation code and grid for NLTE corrections. M.Z. and O.G. aknowledge support by Proyecto Fondecyt Regular ♯1085278. M.Z. and D.M. are partly supported by the BASAL CATA and the FONDAP Center for Astrophysics 15010003.

References

Bensby, T., Feltzing, S., & Lundstrom, I. 2004, A&A, 415, 155
Boothroyd, A. I., & Sackmann, I. J. 1999, ApJ, 510, 232
Brown, J. A., Sneden, C., Lambert, D. L., & Dutchover, E. Jr. 1989, ApJS, 71, 293

Cameron, A. G. W., & Fowler, W. A. 1971, ApJ, 164, 111
Castilho, B. V., Gregorio-Hetem, J., Spite, F., Barbuy, B., & Spite, M. 2000, A&A, 364, 674
Charbonnel, C., & Balachandran, S. C. 2000, A&AS, 359, 563
Charbonnel, C., & do Nacimento 1998, A&AS, 359, 563
Charbonnel, C., & Zahn, J. P. 2007a, A&A, 467, L15
Charbonnel, C., & Zahn, J. P. 2007b, A&A, 476, L29
Costa, J. M., da Silva, L., do Nascimento, J. D., Jr., & De Medeiros, J. R. 2002, A&A, 382, 1016
Cyburt, R. H., Fields, B. D., & Olive, K. A. 2008, JCAP, 11, 012
de La Reza, R., Drake, N. A., & da Silva, L. 1996, ApJ, 456, L115
de La Reza, R., Drake, N. A., da Silva, L., Torres, C. A. O., & Martin, E. L. 1997, ApJ, 482, L77
de Medeiros, J. R., Melo, C. H. F., & Mayor, M. 1996, A&A, 309, 465
Denissenkov, P. A., & Herwig, F. 2004, ApJ, 612, 1081
Denissenkov, P. A., Pinsonneault, M., & MacGregor, K. B. 2009, ApJ, 696, 1823
Domínguez, I., Abia, C., Straniero, O., Cristallo, S., & Pavlenko, Y. V. 2004, A&A, 422, 1045
Drake, N. A., de la Reza, R., da Silva, L., & Lambert, D. L. 2002, AJ, 123, 2703
Faraggiana, R., Gerbaldi, M., Molaro, P., & Lambert, D. L. 1991, MmSAI, 62, 189
Gratton, R. G., & Sneden, C. 1990, A&A, 234, 366
Gratton, R. G., Sneden, C., Carretta, E., & Bragaglia, A. 2000, A&A, 354, 169
Gratton, R., Sneden, C., & Carretta, E. 2004, ARA&A, 42, 385
Gregorio-Hetem, J., Castilho, B. V., & Barbuy, B. 1993, A&A, 268, L25
Grevesse, N., & Sauval, A. J. 1998, Space Sci. Rev., 85, 161
Guandalini, R., Palmerini, M., Busso, M., & Uttenthaler, S. 2009,
Hill, V., & Pasquini, L. 1999, A&A, 348, L21
Iben, I. J. 1967a, ApJ, 147, 624
Iben, I. J. 1967b, ApJ, 147, 650
Jasniewicz, G., Parthasarathy, M., de Laverny, P., & Thevenin, F. 1999, A&A, 342, 831
Jones, M. H. 2008, MNRAS, 387, 845
Kraft, R. P., & Shetrone, M. D. 2000, LIACo, 35, 177
Kurucz, R. L. 1993, CD-ROMs, http://kurucz.harvard.edu
Lecureur, A., Hill, V., Zoccali, M., et al. 2007, A&A, 465, 799
Lind, K., Asplund, M., & Barklem, P. S. 2009a, A&A, 503, 541
Lind, K., Primas, F., Charbonnel, C., Grundahl, F., & Asplund, M. 2009b, A&A, 503, 545
Magain, P. 1984, A&A, 134, 189
McKellar, A. 1940, PASP, 52, 407
Minniti, D., Cook, K. H., Vandehei, T., Alcock, C., & Griest, K. 1998, ApJ, 499, L175
Minniti, D., & Zoccali, M. 2008, IAU Symp., 245, 323
Monaco, L., & Bonifacio, P. 2008, MmSAI, 79, 1
Origlia, L., Rood, R. T., Fabbri, S., et al. 2007, ApJ, 667, L85O
Palacios, A., Charbonnel, C., & Forestini, M. 2001, A&A, 375, L9
Palacios, A., Charbonnel, C., Talon, S., & Siess, L. 2006, A&A, 453, 261
Pilachowski, C. A., Sneden, C., & Hudek, D. 1990, ApJ, 99, 1225
Pilachowski, C. A., Sneden, C., Harmer, D., & Willmarth, D. 2000, ApJ, 119, 2895
Plez, B. 1998, A&A, 337, 495
Pompeia, L., Barbuy, B., Grenon, M., & Castilho, B. V. 2002, ApJ, 570, 820
Ramaty, R., Lingenfelter, R. E., & Kozlovsky, B. 2001, SSRv, 99, 51
Recio-Blanco, A., & de Laverny, P. 2007, A&A, 461, L13
Reddy, B. E., Lambert, D. L., Laws, C., Gonzalez, G., & Covey, K. 2002, MNRAS, 335, 1005
Sackmann, I., & Boothroyd, A. I. 1999, ApJ, 510, 217
Smith, V. V., Plez, B., Lambert, D. L., & Lubowich, D. A. 1995, ApJ, 441, 735
Spite, F., & Spite, M. 1982, A&A, 115, 357
Stetson, P. B., & Pancino, E. 2008, PASP, 120, 1332
Udalski, A., Szymanski, M., Kubiak, M., et al. 2002, Acta Astron., 52, 217
Uttenthaler, S., Lebzelter, T., Palmerini, S., et al. 2007, A&A, 471, L41
Zoccali, M., Cassisi, S., Piotto, G., Bono, G., & Salaris, M. 1999, ApJ, 518, L49
Zoccali, M., Lecureur, A., Barbuy, B., et al. 2006, A&A, 457, L1
Zoccali, M., Lecureur, A., Hill, V., et al. 2008, A&A, 486, 177